Environmental Science & Technology

Article

pubs.acs.org/est

Different Interaction Mechanisms of Eu(III) and ^{243}Am(III) with Carbon Nanotubes Studied by Batch, Spectroscopy Technique and Theoretical Calculation

Xiangxue Wang,[†,‡] Shubin Yang,[*,†,§] Weiqun Shi,[*,∥] Jiaxing Li,[†,§] Tasawar Hayat,[⊥] and Xiangke Wang[*,†,⊥]

[†]School of Environment and Chemical Engineering, North China Electric Power University, Beijing 102206, P. R. China

[‡]Collaborative Innovation Center of Radiation Medicine of Jiangsu Higher Education Institutions, Suzhou, 215123, P. R. China

[§]Key Laboratory of Novel Thin Film Solar Cells, Institute of Plasma Physics, Chinese Academy of Sciences, P.O. Box 1126, Hefei, 230031, P. R. China

[∥]Institute of High Energy Physics, Chinese Academy of Sciences, 100049, Beijing, P. R. China

[⊥]NAAM Research Group, Faculty of Science, King Abdulaziz University, Jeddah 21589, Saudi Arabia

Supporting Information

ABSTRACT: Herein the sorption of Eu(III) and ^{243}Am(III) on multiwalled carbon nanotubes (CNTs) are studied, and the results show that Eu(III) and ^{243}Am(III) could form strong inner-sphere surface complexes on CNT surfaces. However, the sorption of Eu(III) on CNTs is stronger than that of ^{243}Am(III) on CNTs, suggesting the difference in the interaction mechanisms or properties of Eu(III) and ^{243}Am(III) with CNTs, which is quite different from the results of Eu(III) and ^{243}Am(III) interaction on natural clay minerals and oxides. On the basis of the results of density functional theory calculations, the binding energies of Eu(III) on CNTs are much higher than those of ^{243}Am(III) on CNTs, indicating that Eu(III) could form stronger complexes with the oxygen-containing functional groups of CNTs than ^{243}Am(III), which is in good agreement with the experimental results of higher sorption capacity of CNTs for Eu(III). The oxygen-containing functional groups contribute significantly to the uptake of Eu(III) and ^{243}Am(III), and the binding affinity increases in the order of $\equiv S—OH < \equiv S—COOH < \equiv S—COO^-$. This paper highlights the interaction mechanism of Eu(III) and ^{243}Am(III) with different oxygen-containing functional groups of CNTs, which plays an important role for the potential application of CNTs in the preconcentration, removal, and separation of trivalent lanthanides and actinides in environmental pollution cleanup.

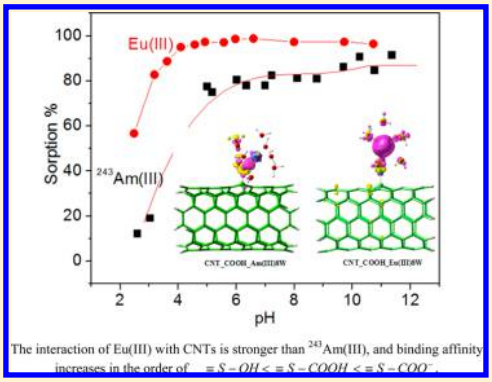

The interaction of Eu(III) with CNTs is stronger than ^{243}Am(III), and binding affinity increases in the order of $\equiv S-OH < \equiv S-COOH < \equiv S-COO^-$

INTRODUCTION

Carbon nanotubes (CNTs) have attracted intense multidisciplinary research due to their outstanding mechanical and electrical properties since they were discovered by Iijima in 1991.[1−4] With regard to the numerous possibilities of various technical applications, it is not surprising that their use for environmental pollution cleanup has also been considered.[5−8] The large BET surface areas of the colloidal CNTs lying in the range of 10−20 m^2/g suggest their possible application as adsorbents for different kinds of environmental pollutants in environmental remediation purposes.[8−12] In the past decade, the application of CNTs as very effective adsorbents for organic and inorganic pollutants has been intensively studied, and the results indicate that CNTs are very suitable materials for the preconcentration of different kinds of pollutants from large volumes of aqueous solutions even at trace level concentrations.[4,11,13−17] The sorption of cationic species is explained by the generation of carbonyl- and carboxylate oxygen-containing functional groups at the CNT surfaces due to the oxidation during nitric acid treatment of the product during their preparation.[10,11,16] The introduced oxygen-containing functional groups could form strong surface complexes with metal ions, and thereby enhances metal ion sorption on CNTs. Those studies reveal the great potential of CNTs for wastewater treatment and remediation of contaminated sites. Although the application of CNTs in the removal of pollutants has been studied extensively, most of the published papers focused on the experimental investigation of environmental pollutant interaction with CNTs combined with modeling analysis. The theoretical calculation on the interaction of environmental pollutants with CNTs is still scarce,[18,19] which is crucial for us to understand the interaction mechanism and for the design and functionalization of CNTs for selective removal

Received: June 1, 2015
Revised: August 13, 2015
Accepted: September 15, 2015
Published: September 15, 2015

DOI: 10.1021/acs.est.5b02679
Environ. Sci. Technol. 2015, 49, 11721−11728

of contaminates from aqueous solutions in environmental pollution cleanup in real applications.

With the development of nuclear energy and in the postprocessing of spent fuels, large amounts of long-lived radionuclides, especially lanthanides and actinides, are generated. Most of the trivalent actinides are long half-life with high radiotoxicity, it is difficult to carry out experimental investigation on the interaction of trivalent actinides with different materials. Among the trivalent actinides, ^{243}Am(III) contributes significantly to the radiotoxicity of nuclear waste because of its high radioactivity and can be released into the natural environment during the processing or disposal.[20,21] In the evaluation of the physicochemical behaviors of trivalent actinides such as ^{243}Am(III) in the natural environment, Eu(III) is usually taken as an analogue of other trivalent actinides because the ionic radius of Eu(III) is almost similar as those of the trivalent lanthanides and actinides.[22,23] The sorption of Eu(III) and ^{243}Am(III) on different kinds of oxides and clay minerals have been studied extensively by batch techniques.[23−27] To the authors' knowledge, for all the published papers about the sorption of Eu(III) and ^{243}Am(III) on minerals and oxides, the Eu(III) and ^{243}Am(III) have very similar sorption properties on the oxides and minerals, which is attributed to the similar ionic radius of Am(III) (1.106 Å for 8-hold coordination) and that of Eu(III) (1.066 Å for 8-hold coordination). The data of Eu(III) interaction with minerals/oxides can be applied to simulate the chemical behavior of ^{243}Am(III) in the natural environment. The batch sorption data were simulated with surface complexation modeling, and the results showed that the sorption was mainly dominated by outer-sphere surface complexation and/or ion exchange at low pH, and by inner-sphere surface complexation and/or surface (co)precipitation at high pH.[26] The interaction mechanism was also evidenced by the spectroscopy analysis such as time-resolved laser fluorescence (TRLFS) spectroscopy and extended X-ray absorption fine structure (EXAFS) spectroscopy.[25,28,29] From the TRLFS study, the hydration number (n_{H2O}) of their aqueous complexes in the first coordination shell could be calculated from the fluorescence decay lifetime. However, Ishida et al.[30] also found that the outer-sphere complex exhibited more rapid fluorescence decay than Eu^{3+} aquo ions, because of the energy transfer to the surface. From the EXAFS analysis, the bond distances and the coordination number could be derived from the spectrum analysis.[25,31] The information are very useful to postulate the species and microstructures of radionuclides on solid surfaces.

Density functional theory (DFT) is a powerful and useful tool for describing and understanding the adsorption reactions.[32−38] Peng et al.[39] used the DFT to calculate the adsorption of NH_3 on graphene oxides (GOs), and the results showed that NH_3 adsorption on GOs was promoted by surface epoxy and hydroxyl functional groups. The interaction of persistent aromatic pollutant with sulfonated graphene was calculated to evidence the high sorption capacity (~2.3−2.4 mmol/g).[40] In our research group,[32,33] the interaction of metal ions (i.e., Pb(II), Ni(II), Sr(II), and U(VI)) on GOs were investigated by batch experiments, spectroscopy analysis and DFT calculations. In addition, we found that the OH-abstracting mechanism was important for the excellent adsorption properties of GOs. However, from the literature query, no theoretical calculations for the investigation of the interaction between trivalent lanthanides/actinides and CNTs with different oxygen-containing functional groups are available, which are crucial for the potential application of CNTs in the removal of lanthanides and actinides in nuclear waste treatment and environmental pollution cleanup.

Because of the outstanding properties of CNTs, the application of CNTs as adsorbents to remove radionuclides from aqueous solutions have been studied extensively, and the results showed that the radionuclides can be preconcentrated efficiently by CNTs.[41−45] Most of the published papers reported the removal of radionuclides by batch experimental study, no work was focused on the comparison of Eu(III) and ^{243}Am(III) on CNTs from experimental and theoretical calculations. Herein, we studied the sorption of Eu(III) and ^{243}Am(III) on CNTs and found that the sorption of Eu(III) on CNTs was stronger than that of ^{243}Am(III) on CNTs, which was quite different from the sorption properties of Eu(III) and ^{243}Am(III) on clay minerals and oxides. We present herein the first time for the comparison of Eu(III) and ^{243}Am(III) interaction with CNTs from experiments and theoretical investigation of Eu(III) and ^{243}Am(III) on CNTs using DFT calculation. The optimal adsorption and orientation of the CNTs−M(III) (Eu(III) and ^{243}Am(III)) complexes were determined, and the binding energies (E_{bd}) between M(III) and CNTs were calculated and analyzed in detail. The theoretical calculation evidenced the differences of Eu(III) and ^{243}Am(III) interaction with CNTs, and the different E_{bd} values of Eu(III)/Am(III) with different oxygen-containing functional groups. The results are crucial for us to understand the interaction mechanism of trivalent Eu(III) and ^{243}Am(III) with CNTs and to functionalize the CNTs for the application in nuclear waste management and radioactive environmental pollution cleanup.

EXPERIMENTAL SECTION

Materials. The CNTs were synthesized by the pyrolysis of iron phthalocyanine and end-opened by oxidation with 3 mol/L HNO_3. The transmission electron microscope (TEM) results revealed that the CNTs were about 1−10 μm long and 10−30 nm outer diameter.[38] Before the experiments, the CNTs were purified carefully by 3 mol/L HNO_3 treatment for oxidation, centrifugation at 18 000 rpm for 40 min, then rinsed with Milli-Q water until the pH reached about 6.0.

Batch Sorption Experiments. All solutions were prepared with Milli-Q water. The sorption of Eu(III) and ^{243}Am(III) on CNTs was investigated at pH 6.1 in 0.1 M $NaClO_4$ by using batch technique. After contact time of 3 days, the solid was separated from liquid phases by ultracentrifugation at 18000 rpm for 35 min. Radionuclides $^{152+154}$Eu(III) and ^{243}Am(III) were used as radiotracers. The concentrations of $^{152+154}$Eu(III) and ^{243}Am(III) were analyzed by Liquid Scintillation counting using a Packard 3100 TR/AB Liquid Scintillation analyzer (PerkinElmer). The scintillation cocktail was ULTIMA GOLD AB (Packard). The distribution coefficient, K_d, was calculated from $K_d = ((C_0 - C_{eq})/C_{eq})\cdot(v/m)$, where C_0 and C_{eq} were the initial and equilibrium concentrations of Eu(III)/^{243}Am(III) in the solution (mol/L), respectively.

TRLFS Analysis. The TRLFS spectra of CNT suspension (m/V = 0.233g/L) containing Eu(III) (1.9×10^{-6} mol/L) were measured using a pulsed Nd:YAG pumped dye laser system (Continuum, Powerlite 9030, ND 6000). The fluorescence emission was detected by an optical multichannel analyzer consisting of a polychromator (Chromex 250) with a 300 lines/mm grating. Laser pulse energy was adjusted to 3 mJ and

DOI: 10.1021/acs.est.5b02679
Environ. Sci. Technol. 2015, 49, 11721−11728

controlled by a photodiode. The CNT suspension containing Eu(III) was directly measured for TRLFS analysis. For measuring the time dependent emission decay, the delay time between laser pulse and camera gating was scanned with time intervals between 10 μs. The emission spectra were recorded at room temperature in the 500−675 nm range, within a constant time window of 1 ms at the constant excitation wavelength of 394 nm.[46]

Kinetic Desorption Study. The chelating cation exchanger (Chelating Resin, 3 M Empore, Switzerland) was converted into a mixed H^+/Na^+ form by rinsing it with 1.0 mol/L HNO_3, washing it with 0.5 mol/L NaCl until the solution pH was near neutral, and finally percolating it with Milli-Q water to remove the excess NaCl.[47] The kinetic desorption of ^{243}Am(III) from CNTs were investigated after 30 days contact time of ^{243}Am-(III) with CNTs at pH 7.3 ± 0.1 and in 0.1 mol/L $NaClO_4$. Then the pH values of the suspensions were lowered to 3.0 and 1.4, respectively. The purified chelating resin containing imminodiacetic acid groups was added to the suspension containing ^{243}Am(III) and CNTs, and the concentration of ^{243}Am(III) remained on CNTs in the suspension was measured after different contact time with Chelating Resin. The pH was maintained by adding 0.01 mol/L $HClO_4$ or NaOH during the experiments.

Computational Calculation Details. In current study, the CNTs used in the experiments have been oxidized by HNO_3 in the pretreatment. According to the previous reports, CNTs could be introduced abundant oxygen-containing functional groups such as —OH, —COO^-, and —COOH by strong acids.[11,48,49] Therefore, herein the oxidized CNTs with —OH, —COOH, and —COO^- groups were employed to describe the adsorption of Eu(III) and ^{243}Am(III) on CNTs. The interactions between M(III) ions and CNTs with different oxygen-containing functional groups as well as the structural and electronic properties of the CNTs−M(III) complexes were calculated by DFT calculation.

The armchair (5, 5) conformations containing 100 carbon atoms are selected as model for CNTs. The oxidized CNTs with —OH, —COOH, and —COO^- groups are denoted as CNT_OH, CNT_COOH, and CNT_COO, respectively (see Figure S1). As Eu(III) and ^{243}Am(III) prefer primary hydration numbers of eight or nine in aqueous solutions,[50−52] eight- or nine-coordinate $M^{III}(H_2O)_n$ noted as M^{III}_nW (n = 8, 8 + 1, or 9) species were employed as the model of M^{III} hydrations. The binding energies (E_{bd}) of M(III) with CNTs were calculated as (E_{bd} = E(CNTs) + E($[M^{III}nW]^{3+}$) − E($[CNTs\_M^{III}nW]^{3+}$)). The more positive value of E_{bd} indicates the stronger binding of M(III) with CNTs. The geometry optimizations and frequency calculations were carried out using the PBE1PBE functional model.[53] The effective core potentials and basis set by Stuttgart−Dresden−Bonn group were used for Eu and Am atoms, 4−31G for CNTs, and 6-31G** was used for —OH, —COOH, and —COO^- groups. The potential energies are refined using larger basis set in which 6-31G** are used for all none metal atoms. To take the solvent effect into account, conductor polarized continuum model[54,55] was employed in the geometry optimization. All calculations were carried out using Gaussian 09 program package.[56]

RESULTS AND DISCUSSION

Experimental sorption of Eu(III) and ^{243}Am(III) on CNTs. The isotherms for Eu(III) and ^{243}Am(III) sorption on CNTs are shown in Figure 1A (batch sorption experiments, pH at 6.1 ± 0.1, in 0.1 M $NaClO_4$, after a contact time of 3 days). It is obvious that the solid/liquid distribution coefficients (K_d) are independent of the Eu(III)/^{243}Am(III) final concentrations. The ideal, linear sorption behavior demonstrates that the sorption of Eu(III)/^{243}Am(III) on CNTs is far from saturation although the content of CNTs is quite low (0.233 g nanotube/L solution). The sorption isotherm of Eu(III) is higher than that of ^{243}Am(III), suggesting the higher interaction ability of CNTs with Eu(III) than ^{243}Am(III), which is not in good agreement with the results of Eu(III) and ^{243}Am(III) sorption on clay minerals and oxides.[27,57] The pH dependence of ^{243}Am(III) and Eu(III) sorption by CNTs ranging from 2.4 to 12 is shown in Figure 1B. In the low pH range, the sorption of ^{243}Am(III) and Eu(III) shows a clear pH dependency, suggesting the interaction with surface sites like carboxylate or hydroxyl groups being progressively deprotonated with increasing pH. At pH ≥ 5, the pH dependence of sorption levels out. More than 96% of Eu(III) and 80% to 92% of ^{243}Am(III) are adsorbed on CNTs at pH > 5.0. Chemisorption is assumed to account for the observed strong ^{243}Am(III) and Eu(III) sorption on CNTs in our experiments rather than physical attachment or electrostatic ion exchange reaction with carboxylate or hydroxyl groups at CNT surfaces.[40,41] This hypothesis is also tested and evidenced by the following spectroscopic study, kinetic desorption experiments and DFT calculations.

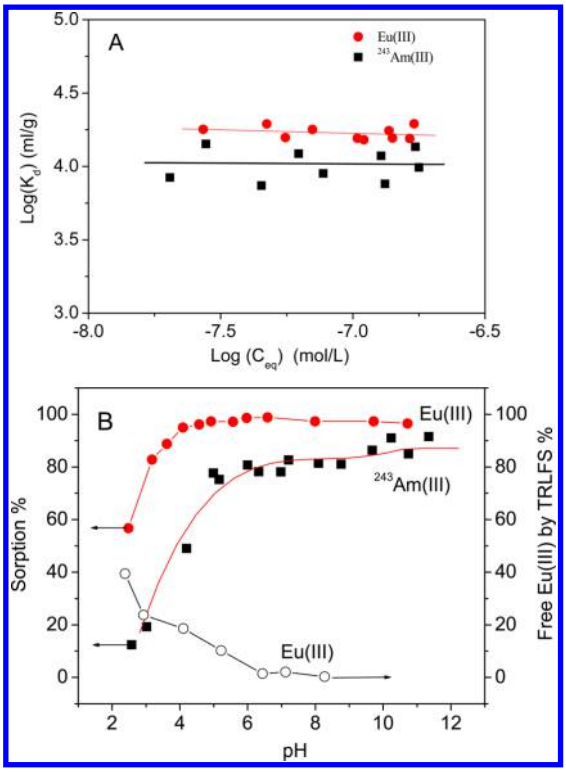

Figure 1. (A) Sorption isotherms for Eu(III) and ^{243}Am(III) to the carbon nanotubes at pH 6.1 in 0.1 M $NaClO_4$, m/V = 0.233g/L. (B) Effect of pH on the sorption of ^{243}Am(III)/Eu(III) to CNTs. The contact time was 3 days. C[^{243}Am(III)] = 4.8 × 10^{-7} mol/L, C[$^{152+154}$Eu(III)] = 4.8 × 10^{-7} mol/L, I= 0.1 M $NaClO_4$, m/V = 0.233g/L. For TRLFS study: C[Eu(III)] = 1.9 × 10^{-6} mol/L, I= 0.1 M $NaClO_4$, m/V = 0.233g/L. The relative concentration of Eu(III) in solution is calculated from the fluorescence intensity and compared to that of the free Eu(III) solution.

DOI: 10.1021/acs.est.5b02679
Environ. Sci. Technol. 2015, 49, 11721−11728

In order to gain insight into the sorption mechanism of Eu(III), TRLFS technique was applied to measure the Eu(III) sorption on CNTs. Chemisorption by inner-sphere surface complex formation is known to have an effect on the intensity and lifetime of Eu(III) fluorescence spectra. The TRLFS spectra of Eu(III) in CNT suspension at different pH values are shown in Figure 2A. The intensity of the spectra decreases with

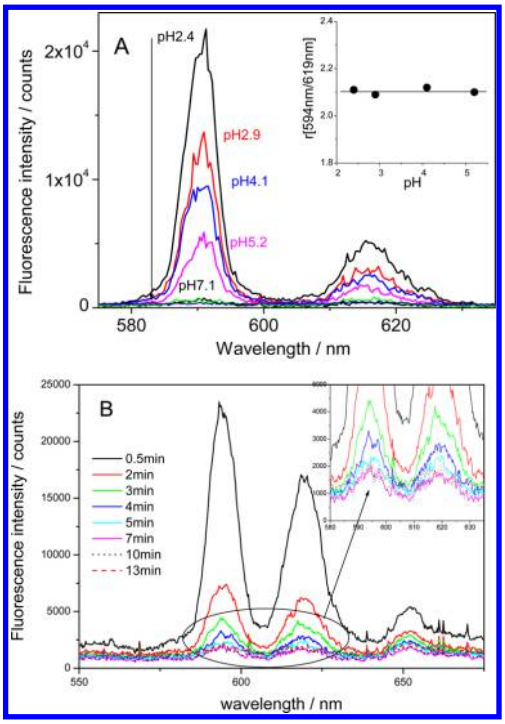

Figure 2. (A) TRLFS spectra of Eu(III) in the presence of carbon nanotubes. C[Eu(III)] = 1.9×10^{-6} mol/L, I = 0.1 M $NaClO_4$, m/V = 0.233g/L. (B) TRLFS study of the time dependent Eu(III) sorption to carbon nanotubes at pH 6.0. C[Eu(III)] = 1.9×10^{-6} mol/L, I = 0.1 M $NaClO_4$, m/V = 0.233g/L.

increasing pH values. The ratio of the intensity of the $^5D_0 \rightarrow {}^7F_1$ transition (λ = 594 nm) to that of $^5D_0 \rightarrow {}^7F_2$ transition (λ = 619 nm) remains constant at 2.1 ± 0.1 with no change in the fluorescence lifetime (~110 μs) (data not shown). The intensity ratio plots as a function of pH was also shown in the inset of Figure 2A. One can see that the intensity ratio vs pH maintains the level under the experimental uncertainties. This finding suggests that only the free Eu(III) ions in the system are detected.[23,25,46] The decrease of the fluorescence intensity indicates static quenching and, thus, indicates the formation of a nonfluorescent Eu(III)-CNT complexes. The concentrations of free Eu(III) ions calculated from the TRLFS analysis in CNT suspensions as a function of contact time is also shown in Figure 1B, one can see that the adsorbed Eu(III) ions cannot be detected by TRLFS, which is attributed to the quenching ability of CNTs for Eu(III) fluorescence properties. Because of the quenching property of CNTs, the surface adsorbed Eu(III) on CNTs cannot be detected by TRLFS. The fluorescence intensity of Eu(III) in the CNT suspension is measured with increasing contact time, and the intensity decreases quickly with increasing contact time (Figure 2B). The ratio of the intensity of $^5D_0 \rightarrow {}^7F_1$ transition to that of $^5D_0 \rightarrow {}^7F_2$ transition remains constant at 2.1 ± 0.1 with increasing contact time under the experimental uncertainties. From the fluorescence intensity variation, it is obvious that the uptake of Eu(III) by CNTs occurs very rapidly and the equilibration is attained within several minutes.

The desorption kinetics of ^{243}Am(III) from CNTs were investigated after one month contact time of ^{243}Am(III) with CNTs (pH at 7.3 ± 0.1, in 0.1 M $NaClO_4$). A purified filter membrane coated with a resin containing imminodiacetic acid groups (Chelating Extraction Disk, 3 M Empore) was added to the solution after previous equilibration with the electrolyte at given pH. Very fast reaction was found for the sorption of free ^{243}Am(III) from solution to the resin in the absence of nanotubes (Figure 3). The results suggest that more than

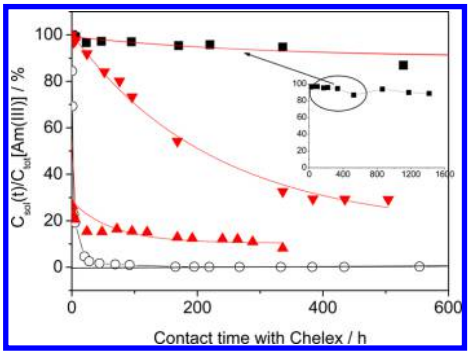

Figure 3. Fractions of ^{243}Am(III) species in a nanotube dispersion as a function of the contact time with a chelating filter resin. The concentration of ^{243}Am(III) is 4×10^{-7} mol/L and that of the nanotubes is 0.233g/L. (■): pH 7.3; (▼): pH 3.0; (▲): pH 1.4; and (○): free Am(III) solution, pH 5.0. The curves are a guide to the eye to show the kinetic desorption of ^{243}Am(III) from CNTs more clearly.

99.99% of free ^{243}Am(III) forms very strong complexes with the chelating resin. In the presence of the nanotubes, the initial ^{243}Am(III) concentration first drops rapidly to ~96% of the initial concentration and then decreases very slowly (Figure 3). The quick sorption of ^{243}Am(III) to chelating resin is attributed to the fast desorption of ^{243}Am(III) from weak sites of CNTs, whereas the kinetic slow desorption of ^{243}Am(III) is due to the dissociation of ^{243}Am(III) from the strong sites of CNTs. The rapid decrease in the beginning is related to the free ^{243}Am(III) ions in solution which are not adsorbed on CNTs. The slow desorption kinetics of ^{243}Am(III) is attributed to the very slow desorption kinetics of ^{243}Am(III) from the CNTs. Even after more than 2 months of contact time, ~ 95% of ^{243}Am(III) still remains bound to CNTs. The experimental results suggest that ^{243}Am(III) forms kinetically stabilized complexes with CNTs and does not desorb from CNTs easily. This finding proves the existence of strong chemical binding to CNTs. After pH adjustment to 3.0, a slower desorption is observed, and about 30% of ^{243}Am(III) are still bound on CNTs even after 10 days of contact time with chelating resin. Comparing those data with sorption data in Figure 1B suggests that only the free ^{243}Am-(III) not bound to CNTs can be scavenged by the chelating resin. Acidification of the dispersion to pH = 1.4, results in a quick but not complete desorption of ^{243}Am(III) from CNTs. The CNTs bound ^{243}Am(III) fraction appears to be kinetically stabilized and does only very slowly dissociate from the CNTs to solution when the equilibration is destroyed. Hummer et al.[58] studied the adsorption of H_2O by uncapped single-walled nanotubes and found that water molecules can enter into the central channels of the nanotubes rapidly by forming hydrogen-bonded chains. We also studied the kinetic desorption of

DOI: 10.1021/acs.est.5b02679
Environ. Sci. Technol. 2015, 49, 11721−11728

Eu(III) from multiwalled carbon nanotubes after the aging time of 4 days and 6 months, respectively, and found that the irreversible fraction of Eu(III) on nanotubes after 6 months was higher than that of Eu(III) on nanotubes after 4 days, suggesting that part of Eu(III) changed from the reversible sites to irreversible sites with increasing aging time.[59] The very slow dissociation kinetics of CNT bound ^{243}Am(III)/Eu(III) could be an indication that the metal ions might form very strong surface complexes with the oxygen-containing functional groups on CNT surfaces, which is also evidenced in the following DFT calculations.

DFT Calculations. Through the DFT calculation, we reveal that (1) how many water moleculars, eight or nine, could coordinate with ^{243}Am(III) or Eu(III) in primary hydration, (2) why the oxidized CNTs have different adsorption characters to ^{243}Am(III) and Eu(III) ions, and (3) which kind of group, —OH, —COOH, or —COO$^-$, is mainly responsible for the adsorption of ^{243}Am(III) and Eu(III). In previous researches,[20,23,60,61] Eu(III) and ^{243}Am(III) are proposed to form cluster with a maximum of 8−9 water molecules in aqueous solutions. Our calculations show that for both ^{243}Am(III) and Eu(III), the 8-water coordinated complex is more stable than 9-water coordinated complexes (see SI). Thus, the 8-water coordinated M(III) complex is used in the calculation of the binding energy of M(III) with CNTs.

The optimized structures of oxidized CNTs−M(III) complexes are shown in Figures S3 and S4. The stable Eu—O and Am—O bonds in the complexes exist, indicating that the oxygen-containing functional groups can form strong surface complexes with Eu(III) or Am(III). Therefore, the strong chemisorptions rather than physical adsorption or ion exchange contributes the Eu(III)/Am(III) adsorption processes. The results of binding energies of the complex systems are calculated and tabulated in Table 1. The E_{bd} values of

Table 1. Binding Energy E_{bd} (kcal/mol) of Oxidized CNTs−M(III) Complexes

oxidized CNTs	M(III)8W	E_{bd} (kcal/mol)	$\varepsilon_{LUMO-HOMO}$ (eV)[a]
CNT_COO$^-$	Am(III)8W	48.3	0.335
CNT_COOH	Am(III)8W	20.2	0.623
CNT_OH	Am(III)8W	7.9	0.634
CNT_COO$^-$	Nd(III)8W	45.2	1.135
CNT_COOH	Nd(III)8W	21.1	1.432
CNT_OH	Nd(III)8W	19.4	1.434
CNT_COO$^-$	Eu(III)8W	58.2	−1.323
CNT_COOH	Eu(III)8W	39.0	−1.034
CNT_OH	Eu(III)8W	30.2	−1.023

[a]The $\varepsilon_{LUMO-HOMO}$ is energy difference between LUMO of M(III)8W and HOMO of oxidized CNTs.

Am_8W with CNT_OH, CNT_COOH, and CNT_COO$^-$ are 7.9, 20.2, and 48.3 kcal/mol, respectively. The same orders of E_{bd} values of Eu_8W with oxidized CNTs are found in the order of CNT_COO$^-$ (58.2 kcal/mol) > CNT_COOH (39.0 kcal/mol) > CNT_OH (30.2 kcal/mol). These results indicate that the —COOH group is mainly responsible for M(III) sorption at low pH values, and with the increase of pH the sorption becomes more stronger due to the deprotonation of —COOH and then the —COO$^-$ group contributes mainly to the uptake of Eu(III) and ^{243}Am(III) to CNTs. Consistently, our experimental results show that the sorption of ^{243}Am(III)/Eu(III) on CNTs increases with pH (see Figure 2).

Compared with ^{243}Am(III), the Eu(III) has much higher E_{bd} values with corresponding oxidized CNTs (see Table 1). These results indicate that the oxidized CNTs prefer the formation of strong surface complexes of Eu(III) to ^{243}Am(III), which is consistent with our batch experimental observations that the removal percentage of Eu(III) is higher than that of ^{243}Am(III). Since the charge transfer interaction is important in the binding process of M(III) to CNTs, the diffence density between the CNT_COO_M(III)8W and its two frangments (CNT_COO$^-$ and M(III)8W) is compared. It is necessary to note that the electron density of Eu(III) increases significantly, but the electron density of ^{243}Am(III) changes little (Figure 4). The results indicate that the charge transfer interaction between Eu(III) and CNT_COO$^-$ is much stronger than that between ^{243}Am(III) and CNT_COO$^-$. The similar results are also found

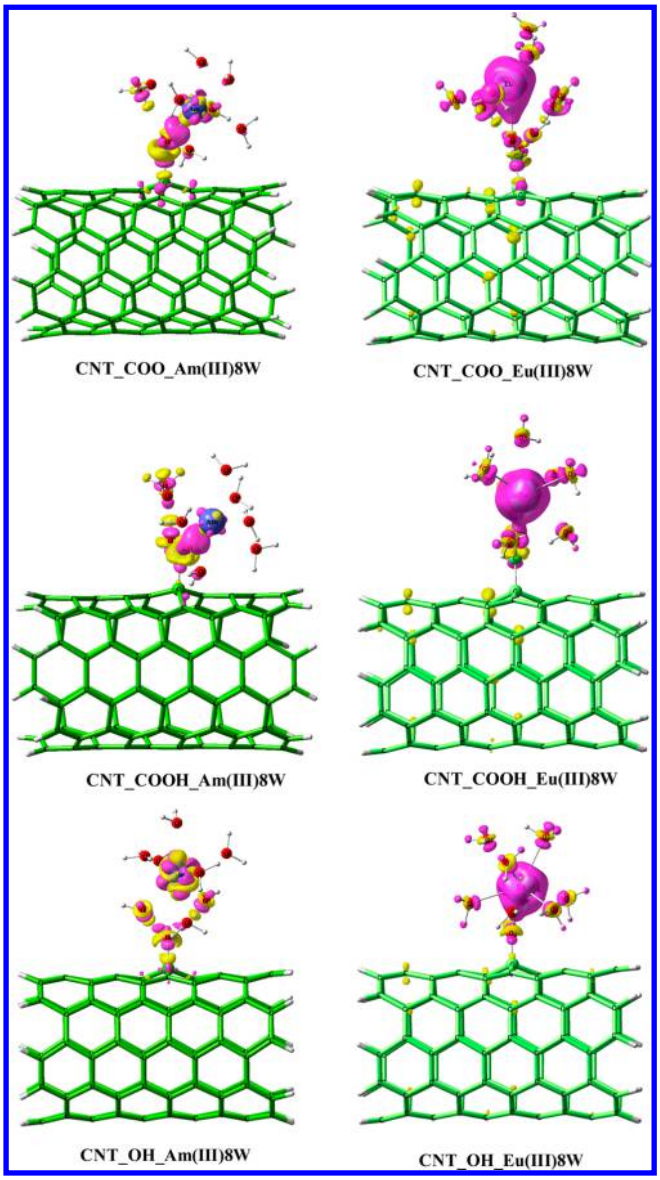

Figure 4. Difference density between the oxidized CNTs_M(III)8W and its two fragments (oxidized CNTs and M(III)8W). The violet color and yellow color represent the increase and decease of electron density, respectively. Both of the colors indicated that the charge transfer interaction is exist. The significant increase electron density indicates the strong charge transfer interaction.

DOI: 10.1021/acs.est.5b02679
Environ. Sci. Technol. 2015, 49, 11721−11728

for the interactions of ^{243}Am(III) and Eu(III) with CNT_OH and CNT_COOH (Figure 4). Because the charge transfer occurs from oxidized CNTs to M(III), the interaction between HOMO of oxidized CNTs and LUMO of M(III)8W is expected to be the key factor for the binding energy. The LUMO energy of Eu(III)8W (−5.611 eV) is much lower than that of Am(III)8W (−3.953 eV). Therefore, the interaction of Eu(III)8W with oxidized CNTs is stronger as compared with that of Am(III)8W with oxidized CNTs (see Scheme 1).

Scheme 1. Charge Transfer Interaction between Oxidized CNTs and M(III)8W

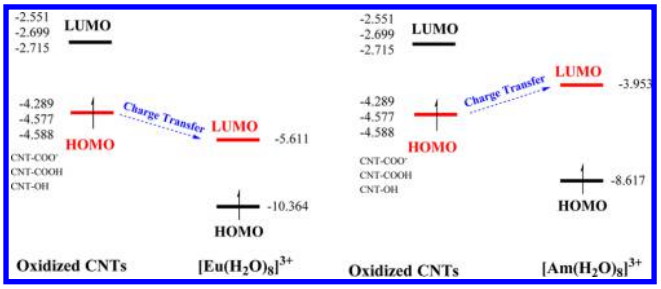

Furthermore, since the HOMO energies (−4.588 eV to −4.289 eV) of all these oxidized CNTs are higher than the LUMO energy of Eu(III)8W (−5.611 eV), the charge transfer from CNTs to Eu(III)8W should be quite easy. As a result, the electron density on Eu(III) increases significantly. Different from Eu(III)8W, the LUMO energy of Am(III)8W (−3.953 eV) is higher than the HOMO energies of oxidized CNTs. Thus, the charge transfer from oxidized CNTs to Am(III)8W is not as strong as that from oxidized CNTs to Eu(III)8W. Likewise, the Eu(III) has higher E_{bd} than Am(III) while interacting with oxidized CNTs (see Scheme 1).

The CNT_COO$^-$ has the highest HOMO energy (−4.289 eV), and the E_{bd} between CNT_COO$^-$ and Eu(III)8W is the largest among these oxidized CNTs; whereas the CNT_OH has the lowest HOMO energy (−4.588 eV) and the interaction between CNT_OH and Eu(III)8W is the weakest. The similar trend can also be found in the interation between differet oxidized CNTs and Am(III)8W that the binding strength order is CNT_COO$^-$ > CNT_COOH > CNT_OH (see Scheme 1 and Table 1). Therefore, the HOMO energies of oxidized CNTs positively correlate with the binding energies. The DFT calculation results are in good agreement with the batch experimental results. On the basis of the DFT calculation, we expect that the modification of oxidized CNTs by introducing strong electron donation groups will facilitate the sorption of trivalent lanthanides and actinides more easily and strongly.

Besides the different electronic energy levels of Eu(III) and ^{243}Am(III) ions, the ionic radius of Am(III) (1.106 Å for 8-hold coordination) is larger than that of Eu(III) (1.066 Å for 8-hold coordination), which can also explain the stronger sorption of Eu(III) on CNTs.[62] In this sense, Nd(III) could be a better homologue of Am(III) as they have more similar properties. The adsorption of Nd(III) by CNTs with different functional groups are also calculated and shown in Figures S5 and S6. The binding energy of Nd(III) is a little smaller than that of Am(III). The LUMO orbital energy of Nd(III) is only 0.82 eV higher than that of Am(III), but higher than that of Eu(III) by 2.48 eV. The result indicates the charge transfer from CNTs to Nd(III) is weaker than to Am(III) and Eu(III). As a result, Nd(III) has the smallest binding energy. Therefore, the coordination with the oxygen-containing functional groups is the main adsorption mechanism of trivalent lanthanides and actinides by CNTs.

In conclusion, the different sorption properties of Eu(III) and ^{243}Am(III) on oxidized CNTs were studied from the batch experiments, and the DFT calculation suggests that the CNT−COO$^-$ forms the strongest surface complexes with Eu(III)8W. The theoretical calculation evidence the differences in the interactions between CNTs with Eu(III) and ^{243}Am(III) ions. The finding in this paper highlights the different binding energies of oxygen-containing functional groups of CNTs with Eu(III) and ^{243}Am(III) ions, which is cruical to understand the interaction mechanism of CNTs with Eu(III) and ^{243}Am(III) ions, and may be helpful for us to functionalize the CNTs for possible separation of trivalent lanthanides and actinides in nuclear waste management, and for the selective preconcentration of long-lived radionuclides from large volumes of aqeuous solutions in environmental radioactive pollution cleanup.

■ ASSOCIATED CONTENT

Supporting Information

The Supporting Information is available free of charge on the ACS Publications website at DOI: 10.1021/acs.est.5b02679.

Additional information for DFT calcualtion, the geometries of M(III)nW species, the DFT-optimized geometries of the complex composed of $Eu^{(III)}(H_2O)_n$ and $Am^{(III)}(H_2O)_n$ (n = 8, 8 + 1) with CNTs (PDF)

■ AUTHOR INFORMATION

Corresponding Authors

*Tel: +86-10-61772890; fax: +86-10-61772890; e-mail: xkwang@ipp.ac.cn or xkwang@ncepu.edu.cn (X.W.).
*E-mail: sdysb2006@163.com (S.Y.).
*E-mail: shiwq@ihep.ac.cn (W.S.).

Notes

The authors declare no competing financial interest.

■ ACKNOWLEDGMENTS

One of the authors (X.K.W.) acknowledges the support from the Alexander von Humboldt (AvH) Foundation for a Research Fellowship in Karlsruhe Research Center, and the favorable discussion with Prof. H. Geckeis and Dr. Th. Rabung to improve the quality of this manuscript. Financial support from National Natural Science Foundation of China (21577032; 21225730; 91326202; 41273134), the Fundamental Research Funds for the Central Universities (JB2015001), the Jiangsu Provincial Key Laboratory of Radiation Medicine and Protection, the Priority Academic Program Development of Jiangsu Higher Education Institutions, and MCTL Visiting Fellowship Program from Key Laboratory of Marine Chemistry Theory and Technology (Ocean University of China), Ministry of Education are acknowledged.

■ REFERENCES

(1) Iijima, S. Helical microtubules of graphitic carbon. *Nature* **1991**, *354*, 56−58.

(2) Strano, M. S.; Dyke, C. A.; Usrey, M. L.; Barone, P. W.; Allen, M. J.; Shan, H.; Kittrell, C.; Hauge, R. H.; Tour, J. M.; Smalley, R. E. Electronic Structure Control of Single-Walled Carbon Nanotube Functionalization. *Science* **2003**, *301*, 1519−1522.

(3) Lou, X.; Detrembleur, C.; Pagnoulle, C.; Jérôme, R.; Bocharova, V.; Kiriy, A.; Stamm, M. Surface Modification of Multiwalled Carbon

DOI: 10.1021/acs.est.5b02679
Environ. Sci. Technol. 2015, 49, 11721−11728

Nanotubes by Poly(2-vinylpyridine): Dispersion, Selective Deposition, and Decoration of the Nanotubes. *Adv. Mater.* **2004**, *16*, 2123−2127.
(4) Long, R. Q.; Yang, R. T. Carbon nanotubes as superior sorbent for dioxin removal. *J. Am. Chem. Soc.* **2001**, *123*, 2058−2059.
(5) Zhang, M. G.; Gorski, W. Electrochemical sensing based on redox mediation at carbon nanotubes. *Anal. Chem.* **2005**, *77*, 3960−3965.
(6) Zhang, M. G.; Gorski, W. Electrochemical sensing platform based on the carbon nanotubes/redox mediators-biopolymer system. *J. Am. Chem. Soc.* **2005**, *127*, 2058−2059.
(7) Stankovich, S.; Dikin, D. A.; Dommett, G. H. B.; Kohlhaas, K. M.; Zimney, E. J.; Stach, E. A.; Piner, R. D.; Nguyen, S. T.; Ruoff, R. S. Graphene-based composite materials. *Nature* **2006**, *442*, 282−286.
(8) Premkumar, T.; Mezzenga, R.; Geckeler, K. E. Carbon nanotubes in the liquid phase: addressing the issue of dispersion. *Small* **2012**, *8* (9), 1299−1313.
(9) Rao, G. P.; Lu, C.; Su, F. Sorption of divalent metal ions from aqueous solution by carbon nanotubes: A review. *Sep. Purif. Technol.* **2007**, *58*, 224−231.
(10) Li, J.; Chen, C. L.; Zhang, S. W.; Ren, X. M.; Tan, X. L.; Wang, X. K. Critical Evaluation of Adsorption-Desorption Hysteresis of Heavy Metal Ions from Carbon Nanotubes: Influence of Wall Number and Surface Functionalization. *Chem. - Asian J.* **2014**, *9*, 1144−1151.
(11) Xu, D.; Tan, X.; Chen, C.; Wang, X. Removal of Pb(II) from aqueous solution by oxidized multiwalled carbon nanotubes. *J. Hazard. Mater.* **2008**, *154*, 407−416.
(12) Ren, X. M.; Chen, C. L.; Nagatsu, M.; Wang, X. K. Carbon nanotubes as adsorbents in environmental pollution management: A review. *Chem. Eng. J.* **2011**, *170*, 395−410.
(13) Kandah, M. I.; Meunier, J. L. Removal of nickel ions from water by multi-walled carbon nanotubes. *J. Hazard. Mater.* **2007**, *146*, 283−288.
(14) Yang, S. B.; Hu, J.; Chen, C. L.; Shao, D. D.; Wang, X. K. Mutual effects of Pb(II) and humic acid adsorption on multiwalled carbon nanotubes/polyacrylamide composites from aqueous solutions. *Environ. Sci. Technol.* **2011**, *45*, 3621−3627.
(15) Pan, B.; Xing, B. Adsorption Mechanisms of Organic Chemicals on Carbon Nanotubes. *Environ. Sci. Technol.* **2008**, *42*, 9005−9013.
(16) Yang, S.; Li, J.; Shao, D.; Hu, J.; Wang, X. Adsorption of Ni(II) on oxidized multi-walled carbon nanotubes: effect of contact time, pH, foreign ions and PAA. *J. Hazard. Mater.* **2009**, *166*, 109−116.
(17) Wu, W.; Jiang, W.; Zhang, W.; Lin, D.; Yang, K. Influence of Functional Groups on Desorption of Organic Compounds from Carbon Nanotubes into Water: Insight into Desorption Hysteresis. *Environ. Sci. Technol.* **2013**, *47*, 8373−8382.
(18) Hossein, T.; Dana, S. DFT, QTAIM, and NBO study of adsorption of rare gases into and on the surface of sulfur-doped, single-wall carbon nanotubes. *J. Phys. Chem. C* **2015**, *119*, 6502−6510.
(19) Hossein, T.; Fahimeh, H. Adsorption of molecular iodine on the surface of sulfur-doped carbon nanotubes: theoretical study on their interactions, sensor properties and other applications. *Struct. Chem.* **2015**, *26*, 151−158.
(20) Lan, J. H.; Shi, W. Q.; Yuan, L. Y.; Feng, Y. X.; Zhao, Y. L.; Chai, Z. F. Thermodynamic Study on the Complexation of Am(III) and Eu(III) with Tetradentate Nitrogen Ligands: A Probe of Complex Species and Reactions in Aqueous Solution. *J. Phys. Chem. A* **2012**, *116*, 504−511.
(21) Romanchuk, A. Y.; Slesarev, A. S.; Kalmykov, S. N.; Kosynkin, D. V.; Tour, J. M. Graphene oxide for effective radionuclide removal. *Phys. Chem. Chem. Phys.* **2013**, *15*, 2321−2327.
(22) Xi, J.; Lan, J. H.; Lu, G. W.; Zhao, Y. L.; Chai, Z. F.; Shi, W. Q. A density functional theory study of complex species and reactions of Am(III)/Eu(III) with nitrate anions. *Mol. Simul.* **2014**, *40*, 379−386.
(23) Tan, X.; Fang, M.; Wang, X. Sorption speciation of lanthanides/actinides on minerals by TRLFS, EXAFS and DFT studies: a review. *Molecules* **2010**, *15*, 8431−8468.
(24) Sun, Y.; Chen, C.; Tan, X.; Shao, D.; Li, J.; Zhao, G.; Yang, S.; Wang, Q.; Wang, X. Enhanced adsorption of Eu(III) on mesoporous Al_2O_3/expanded graphite composites investigated by macroscopic and microscopic techniques. *Dalton Trans.* **2012**, *41*, 13388−13394.
(25) Tan, X. L.; Wang, X. K.; Geckeis, H.; Rabung, T. Sorption of Eu(III) on humic acid or fulvic acid bound to hydrous alumina studied by SEM-EDS, XPS, TRLFS, and batch techniques. *Environ. Sci. Technol.* **2008**, *42*, 6532−6537.
(26) Sun, Y.; Li, J.; Wang, X. The retention of uranium and europium onto sepiolite investigated by macroscopic, spectroscopic and modeling techniques. *Geochim. Cosmochim. Acta* **2014**, *140*, 621−643.
(27) Wang, X. X.; Li, J. X.; Dai, S. Y.; Hayat, Y.; Alsaedi, A.; Wang, X. K. Interactions of Eu(III) and ^{243}Am(III) on humic acid-bound γ-Al_2O_3 studied by batch and kinetic dissociation techniques. *Chem. Eng. J.* **2015**, *273*, 588−594.
(28) Wang, X. X.; Sun, Y. B.; Wang, X. K. Interaction mechanism of Eu(III) with MX-80 bentonite studied by batch, TRLFS and kinetic desorption techniques. *Chem. Eng. J.* **2015**, *264*, 570−576.
(29) Sun, Y.; Wang, Q.; Chen, C.; Tan, X.; Wang, X. Interaction between Eu(III) and Graphene Oxide Nanosheets Investigated by Batch and Extended X-ray Absorption Fine Structure Spectroscopy and by Modeling Techniques. *Environ. Sci. Technol.* **2012**, *46*, 6020−6027.
(30) Ishida, K.; Saito, T.; Aoyagi, N.; Kimura, T.; Nagaishi, R.; Nagasaki, S.; Tanaka, S. Surface speciation of Eu^{3+} adsorbed on kaolinite by time-resolved laser fluorescence spectroscopy (TRLFS) and parallel factor analysis (PARAFAC). *J. Colloid Interface Sci.* **2012**, *374*, 258−266.
(31) Yang, S. T.; Sheng, G. D.; Montavon, G.; Guo, Z. Q.; Tan, X. L.; Grambow, B.; Wang, X. K. Investigation of Eu(III) immobilization on γ-Al_2O_3 surfaces by combining batch technique and EXAFS analysis: Role of contact time and humic acid. *Geochim. Cosmochim. Acta* **2013**, *121*, 84−104.
(32) Yang, S.; Chen, C.; Chen, Y.; Li, J.; Wang, D.; Wang, X.; Hu, W. Competitive Adsorption of Pb^{II}, Ni^{II}, and Sr^{II} Ions on Graphene Oxides: A Combined Experimental and Theoretical Study. *ChemPlusChem* **2015**, *80*, 480−484.
(33) Sun, Y. B.; Yang, S. B.; Chen, Y.; Ding, C. C.; Cheng, W. C.; Wang, X. K. Adsorption and Desorption of U(VI) on Functionalized Graphene Oxides: a Combined Experimental and Theoretical Study. *Environ. Sci. Technol.* **2015**, *49*, 4255−4262.
(34) Boukhvalov, D. W.; Katsnelson, M. I. Modeling of Graphite Oxide. *J. Am. Chem. Soc.* **2008**, *130*, 10697−10701.
(35) Jung, I.; Dikin, D. A.; Piner, R. D.; Ruoff, R. S. Tunable Electrical Conductivity of Individual Graphene Oxide Sheets Reduced at "Low" Temperatures. *Nano Lett.* **2008**, *8*, 4283−4287.
(36) Boukhvalov, D. W. DFT modeling of the covalent functionalization of graphene: from ideal to realistic models. *RSC Adv.* **2013**, *3*, 7150−7159.
(37) Chen, Y.; Sakaki, S. Theoretical study of mononuclear nickel(I), nickel(0), copper(I), and cobalt(I) dioxygen complexes: new insight into differences and similarities in geometry and bonding nature. *Inorg. Chem.* **2013**, *52*, 13146−13159.
(38) Lin, Z.; Chen, Y.; Li, X.; Fang, W. Pb^{2+} induced DNA conformational switch from hairpin to G-quadruplex: electrochemical detection of Pb^{2+}. *Analyst* **2011**, *136*, 2367−2372.
(39) Peng, Y.; Li, J. Ammonia adsorption on graphene and graphene oxide: a first-principles study. *Front. Environ. Sci. Eng.* **2013**, *7*, 403−411.
(40) Zhao, G. X.; Jiang, L.; He, Y. D.; Li, J. X.; Dong, H. L.; Wang, X. K.; Hu, W. P. Sulfonated Graphene for Persistent Aromatic Pollutant Management. *Adv. Mater.* **2011**, *23*, 3959−3963.
(41) Wang, X. K.; Chen, C. L.; Hu, W. P.; Ding, A. P.; Xu, D.; Zhou, X. Sorption of ^{243}Am(III) to Multi-wall Carbon Nanotubes. *Environ. Sci. Technol.* **2005**, *39*, 2856−2860.
(42) Chen, C. L.; Hu, J.; Xu, D.; Tan, X. L.; Meng, Y. D.; Wang, X. K. Surface Complexation Modeling of Sr(II) and Eu(III) Adsorption onto Oxidized Multiwall Carbon Nanotubes. *J. Colloid Interface Sci.* **2008**, *323*, 33−41.
(43) Chen, C. L.; Wang, X. K.; Nagatsu, M. Europium Adsorption on Multiwall Carbon Nanotube/Iron Oxide Magnetic Composite in the Presence of Polyacrylic Acid. *Environ. Sci. Technol.* **2009**, *43*, 2362−2367.

DOI: 10.1021/acs.est.5b02679
Environ. Sci. Technol. 2015, 49, 11721−11728

(44) Shao, D. D.; Jiang, Z. Q.; Wang, X. K.; Li, J. X.; Meng, Y. D. Plasma induced grafting carboxymethyl cellulose on multiwalled carbon nanotubes for the removal of UO_2^{2+} from aqueous solution. *J. Phys. Chem. B* **2009**, *113*, 860−864.
(45) Belloni, F.; Kutahyali, C.; Rondinella, V. V.; Carbol, P.; Wiss, T.; Mangione, A. Can carbon nanotubes play a role in the field of nuclear waste management? *Environ. Sci. Technol.* **2009**, *43*, 1250−1255.
(46) Rabung, Th.; Stumpf, Th.; Geckeis, H.; Klenze, R.; Kim, J. I. Sorption of Am(III) and Eu(III) onto γ-alumina: experiment and modeling. *Radiochim. Acta* **2000**, *88*, 711−716.
(47) Geckeis, H.; Rabung, Th.; Ngo Mann, T.; Kim, J. I.; Beck, H. P. Humic colloid-borne natural polyvalent metal ions: dissociation experiment. *Environ. Sci. Technol.* **2002**, *36*, 2946−2952.
(48) Hu, J.; Chen, C.; Zhu, X.; Wang, X. Removal of chromium from aqueous solution by using oxidized multiwalled carbon nanotubes. *J. Hazard. Mater.* **2009**, *162*, 1542−1550.
(49) Sun, Y.; Yang, S.; Sheng, G.; Guo, Z.; Wang, X. The removal of U(VI) from aqueous solution by oxidized multiwalled carbon nanotubes. *J. Environ. Radioact.* **2012**, *105*, 40−47.
(50) Antonio, M. R.; Williams, C. W.; Soderholm, L. Berkelium redox speciation. *Radiochim. Acta* **2002**, *90*, 851−856.
(51) D'Angelo, P.; Martelli, F.; Spezia, R.; Filipponi, A.; Denecke, M. A. Hydration properties and ionic radii of actinide(III) ions in aqueous solution. *Inorg. Chem.* **2013**, *52*, 10318−10324.
(52) Revel, R.; Den Auwer, C.; Madic, C.; David, F.; Fourest, B.; Hubert, S.; Le Du, J. F.; Morss, L. R. First Investigation on the L Edges of the 249Cf Aquo Ion by X-ray Absorption Spectroscopy. *Inorg. Chem.* **1999**, *38*, 4139−4141.
(53) Perdew, J. P.; Burke, K.; Ernzerhof, M. Generalized Gradient Approximation Made Simple. *Phys. Rev. Lett.* **1996**, *77*, 3865−3868.
(54) Cossi, M.; Barone, V.; Robb, M. A. A direct procedure for the evaluation of solvent effects in MC-SCF calculations. *J. Chem. Phys.* **1999**, *111*, 5295−5302.
(55) Cossi, M.; Rega, N.; Scalmani, G.; Barone, V. Energies, structures, and electronic properties of molecules in solution with the C-PCM solvation model. *J. Comput. Chem.* **2003**, *24*, 669−681.
(56) Frisch, M. J.; Trucks, G. W.; Schlegel, H. B.; Scuseria, G. E.; Robb, M. A.; Cheeseman, J. R.; Scalmani, G.; Barone, V.; Mennucci, B.; Petersson, G. A.; Nakatsuji, H.; Caricato, M.; Li, X.; Hratchian, H. P.; Izmaylov, A. F.; Bloino, J.; Zheng, G.; Sonnenberg, J. L.; Hada, M.; Ehara, M.; Toyota, K.; Fukuda, R.; Hasegawa, J.; Ishida, M.; Nakajima, T.; Honda, Y.; Kitao, O.; Nakai, H.; Vreven, T.; Montgomery, J. A., Jr.; Peralta, J. E.; Ogliaro, F.; Bearpark, M.; Heyd, J. J.; Brothers, E.; Kudin, K. N.; Staroverov, V. N.; Kobayashi, R.; Normand, J.; Raghavachari, K.; Rendell, A.; Burant, J. C.; Iyengar, S. S.; Tomasi, J.; Cossi, M.; Rega, N.; Millam, J. M.; Klene, M.; Knox, J. E.; Cross, J. B.; Bakken, V.; Adamo, C.; Jaramillo, J.; Gomperts, R.; Stratmann, R. E.; Yazyev, O.; Austin, A. J.; Cammi, R.; Pomelli, C.; Ochterski, J. W.; Martin, R. L.; Morokuma, K.; Zakrzewski, V. G.; Voth, G. A.; Salvador, P.; Dannenberg, J. J.; Dapprich, S.; Daniels, A. D.; Farkas, O.; Foresman, J. B.; Ortiz, J. V.; Cioslowski, J.; Fox, D. J. *Gaussian 09*, revision A.02; Gaussian, Inc.: Wallingford, CT, 2009.
(57) Fan, Q. H.; Zhang, M. L.; Zhang, Y. Y.; Ding, K. F.; Yang, Z. Q.; Wu, W. S. Sorption of Eu(III) and Am(III) on attapulgite: effect of pH, ionic strength and fulvic acid. *Radiochim. Acta* **2010**, *98*, 19−25.
(58) Hummer, G.; Rasaiah, J. C.; Noworyta, J. P. Water conduction through the hydrophobic channel of a carbon nanotube. *Nature* **2001**, *414*, 188−190.
(59) Tan, X. L.; Xu, D.; Chen, C. L.; Wang, X. K.; Hu, W. P. Adsorption and kinetic desorption study of $^{152+154}$Eu(III) on multiwall carbon nanotubes from aqueous solution by using chelating resin and XPS methods. *Radiochim. Acta* **2008**, *96*, 23−29.
(60) Wiebke, J.; Moritz, A.; Cao, X.; Dolg, M. Approaching actinide(+III) hydration from first principles. *Phys. Chem. Chem. Phys.* **2007**, *9*, 459−465.
(61) Xiao, C. L.; Wang, C. Z.; Lan, J. H.; Yuan, L. Y.; Zhao, Y. L.; Chai, Z. F.; Shi, W. Q. Selective separation of Am(III) from Eu(III) by 2,9-Bis(dialkyl-1,2,4-triazin-3-yl)-1,10-phenanthrolines: a relativistic quantum chemistry study. *Radiochim. Acta* **2014**, *102*, 875−886.
(62) Choppin, G. R.; Rizkalla, E. N. Solution chemistry of actinides and lanthanides. In *Handbook on the Physics and Chemistry of Rare Earths*; Elsevier: New York, 1994; Vol. *18*, pp 559−590.

DOI: 10.1021/acs.est.5b02679
Environ. Sci. Technol. 2015, 49, 11721−11728